TAO, Vol.5, No.4, 443-461, December 1994

Numerical and Physical Experiments on Dynamic Properties of Elastic Body Waves at the Boundary With Non-rigid Contact Between Media

MARGARITA LUNEVA[1,2], CHENGSUNG WANG[1], YOUNG FO CHANG[3], and CHAO-HUI HSIEH[3]

(Manuscript received 17 November 1993, in final form 19 July 1994)

ABSTRACT

Dynamic interpretation of seismic waves is traditionally based on the model of geological medium as a combination of layers and blocks bonded rigidly to each other. However, a discrepancy has been found between the accumulated theoretical data and experimental data in seismic wave dynamics. Geophysical and rheological study of the Earth's crustal structure has indicated an important role of layering and fracturing. So, some boundaries in the Earth's crust can be treated as a non-rigid contact between media, i.e., as a mechanically weakened contact or with thin intermediary layer filled with loose or viscous materials. The theory of non-rigid contact between media has been developed in the literature, but the study of the dynamic characteristics of waves generated at a boundary with non-rigid contact is still required. Here we present the results of numerical and physical ultrasonic experiments on the reflected and transmitted seismic body wave dynamics for the model of non-rigid contact at the boundary between isotropic elastic media. These calculations are based on the non-rigid contact theory which is defined by the boundary conditions with discontinuities of the tangent and normal components of time derivative of the displacement vector across the interface. Our results demonstrate that the amplitude and phase behavior of the generated waves at the non-rigid contact is considerably different from those at the rigid contact between media. The physical ultrasonic experiment was performed for a model of a single fracture on a sheet of duraluminium with a thin filled-plasticine layer. The comparison of physical experimental data with theoretical computations shows a high level of agreement.

(Key words: Elastic body waves, Non-rigid contact between media, Reflection/Trasmission coefficients)

[1] Department of Oceanography, National Taiwan Ocean University, Keelung, Taiwan, R.O.C.

[2] Institute of Tectonics and Geophysics, Far East Branch of Russian Academy of Sciences, 65 Kim-Yu-Chen St., Khabarovsk, Russia

[3] Institute of Geophysics, National Central University, Chung-Li, Taiwan, R.O.C.

1. INTRODUCTION

Modern experimental and theoretical investigations of physical properties of the Earth's materials show that within the Earth's crust the rocks are brittle with fractures (e.g., Brace *et al.*, 1966; Byerlee, 1968; Nikolaevsky, 1983). Seismic velocity profiles reflect general relationships between changes in wave dynamics with depth and changes in the character of fracturing. Seismic boundaries can also have a complex nature and correspond not only to the alternation of rock types. Deep drill-hole data in the Kola peninsula (Kozlovsky, 1984) show that sheets of different composition cross the observed seismic boundaries at an angle, while the boundaries of metamorphism alternation (fracture healing and material reworking under conditions of high pressure and temperature) are parallel to these. The data also show that the area of the Conrad discontinuity is represented by a zone of fractures with internal waters traveling between them. According to numerous detailed seismic data, the Moho discontinuity is presented as a series of layers that may reflect the alternation of physical-chemical transitional processes in this zone (e.g., Malamud and Nikolaevsky, 1989). Therefore some seismic boundaries can be treated as interfaces with non-rigid contact between media, which can be represented by weakened layers caused by mechanical or by physical-chemical processes, when the thickness of the layer is much smaller than the wavelength and the values of seismic velocities in the layer are much smaller than those in the contacting media. The solution of the elasto-dynamic equations for waves incident upon a thin layer was given by Pod'yapolsky (1963). He showed that the boundary condition of non-rigid contact at the boundary of two half-spaces can be deduced from the conditions of rigid contact of a thin fluid-filled layer and two half-spaces. In this case, the tangent component of the displacement has discontinuity. The value of the discontinuity is proportional to the tangent component of applied stress and to the limit of the ratio of the layer's thickness to the shear wave velocity. Klem-Musatov (1965) developed this theory for general situation where neither tangent nor normal displacement components are continuous. Using these conditions the effective elastic moduli and the analytical formulas for the velocity values of transverse-isotropic medium (equivalent to the fractured medium) have been found (Aizenberg *et al.*, 1974). Almost the same theoretical results were obtained by Schoenberg (1980) and tested experimentally for the fractured medium model (Hsu and Schoenberg, 1993; Pyrak-Nolte *et al.*, 1990b). Field and laboratory experiments detect the particular behavior of the amplitudes and the waveforms of waves generated by single fractures (Lutsh, 1959, Yu and Telford, 1973; Kleinberg *et al.*, 1982, Pyrak-Nolte *et al.*, 1990a). Yanovskaya and Dmitrieva (1991) considered the Moho boundary as an interface with non-rigid contact in order to explain the strong amplitudes of the reflected and transmitted converted waves generated at this boundary. The purposes of this paper are to examine the behavior of the reflection and transmission coefficients of elastic body waves for the model of the non-rigid contact at the boundary between isotropic elastic media and to compare with those for the rigid contact. The reflection and transmission coefficients were calculated as a function of the propagation directions for the P and SV incident waves and for the different non-rigidity parameters' values. Also, a 2-D physical ultrasonic experiment was performed on a sheet of duraluminium with a thin plasticine-filled layer to check the theory of non-rigid contact between media. We present the results of the comparison of experimental seismograms and reflection/transmission coefficients with those results predicted theoretically.

2. THEORY

In physical terms, the model of a fracture may be represented as an interface of weakened mechanical contact between two media or as a thin layer filled with loose or viscous material, when the thickness of the layer is much smaller than the wavelength of the incident wave. The asymptotic ray theory has restrictions in the evaluation of dynamic properties of waves generated by a thin layer, because the layer's thickness must exceed the wavelength of the incident wave and the conditions of rigid contact must be satisfied at the interface between media (continuity of the displacement and stress must be attained across the interface). To eliminate this restriction Pod'yapolsky (1963) deduced that, in the limit, the conditions of a thin layer's and two half-spaces' rigid contact can be transformed into the conditions of non-rigid contact of two half-spaces. In this limit case, both the layer thickness and the shear wave velocity tend to zero, but at the same time, their ratio is different from zero. Thus, in a 2-D rectangular coordinate system (x, z) with a plane interface (z =constant) between two elastic isotropic homogeneous media, the boundary conditions of non-rigid contact for the harmonic plane incident wave can be defined as:

$$\begin{cases} \sigma_{zz1} = \sigma_{zz2} \\ \sigma_{zx1} = \sigma_{zx2} \\ U_{z1} = U_{z2} \\ U_{x1} + (\lim\limits_{\substack{h \to 0 \\ \mu \to 0}} h/\mu)\sigma_{zx1} = U_{x2} \end{cases}, \tag{1}$$

where U_x and Uz are the horizontal and vertical components of the displacement vector, and σ_{zx} and σ_{zz} are the horizontal and vertical components of the stress tensor. Parameter h is the thickness of the layer and μ is Lame's constant of the layer. Indices 1, 2 specify the upper and lower half-spaces, respectively. The horizontal component of the displacement vector has a discontinuity whose magnitude is proportional to the value of the horizontal component of the stress tensor and to the value of h/μ. From the physical point of view, the requirement $h \to 0$ means that h must be much smaller than the wavelength of the incident wave, and requirement $\mu \to 0$ means that this parameter in a thin layer must be much smaller than the same parameter in the surrounding half-spaces.

A more general model of non-rigid contact was proposed by Klem-Musatov (1965), in which both the horizontal and vertical components of the partial time derivative of the displacement vector are not continuous across the interface. So, more general conditions of non-rigid contact are expressed in case of stationary oscillations as follows:

$$\begin{cases} \sigma_{zz1} = \sigma_{zz2} \\ \sigma_{zx1} = \sigma_{zx2} \\ \frac{\partial U_{x1}}{\partial t} - \frac{\partial U_{x2}}{\partial t} = \Lambda_s \sigma_{zx2}, \\ \frac{\partial U_{z1}}{\partial t} - \frac{\partial U_{z2}}{\partial t} = \Lambda_p \sigma_{zz2} \end{cases} \tag{2}$$

where Λ_p and Λ_s are the longitudinal and transverse parameters of non-rigidity, which are complex -valued with dimension length/(stress$\times$ time) - (m^2s/kg) (Klem-Musatov, 1965). The boundary conditions (2) characterize the possibility of "slipping" and "interpenetrating" of one medium into another; and the degree of these effects depends on the value of parameters

Λ_p and Λ_s. If $\Lambda_p = 0$ and $\Lambda_s = 0$, this case is of a rigid contact. The parameters of non-rigidity can be obtained only experimentally. They are dependent on the physical parameters of the layer, the layer's thickness, and the frequency of the incident wave. In general, Λ_p and Λ_s are defined as:

$$\Lambda_\nu = \frac{ik_\nu h}{\rho v_\nu} g(k_\nu h, v_\nu, \rho); \quad \nu = p, s; \quad i = \sqrt{-1} \tag{3}$$

ρ is the layer's density, v_ν is the layer's wave velocity, and k_ν is the wave number. Function g defines a specific model of the contact.

The complete solution of the system of equations for the boundary conditions (2), after substitution of the displacement, can be rewritten in matrix form (Aizenberg *et al.*, 1974; Druzhinin and Luneva, 1992):

$$\mathbf{CK=B} \tag{4}$$

$$\mathbf{K} = (K_{\nu 1}^{p1} \quad K_{\nu 1}^{s1} \quad K_{\nu 1}^{p2} \quad K_{\nu 1}^{s2})^T, \qquad \nu = p, s,$$

where **K** is the vector-column of unknown reflection and transmission coefficients. The upper indices show the type of generated wave and the number of medium (1-reflection; 2-transmission); the lower indices show the type of incident wave (P, SV), which goes from the first medium. Matrices **C** and **B** may be represented in the common form:

$$\mathbf{B}_{v=p} = \begin{pmatrix} -W_{p1} cos2\Theta_{s1} \\ W_{p1}\gamma_1^2 sin2\Theta_{p1} \\ cos\Theta_{p1} \\ -sin\Theta_{p1} \end{pmatrix}, \quad \mathbf{B}_{v=s} = \begin{pmatrix} W_{p1}\gamma_1 sin2\Theta_{s1} \\ W_{p1}\gamma_1 cos2\Theta_{s1} \\ -sin\Theta_{s1} \\ -cos\Theta_{s1} \end{pmatrix},$$

$$\mathbf{C} = \begin{pmatrix} W_{p1} cos2\Theta_{s1} & W_{p1}\gamma_1 sin2\Theta_{s1} & -W_{p2} cos2\Theta_{s2} & W_{p2}\gamma_2 sin2\Theta_{s2} \\ W_{p1}\gamma_1^2 sin2\Theta_{p1} & -W_{p1}\gamma_1 cos2\Theta_{s1} & W_{p2}\gamma_2^2 sin2\Theta_{p2} & W_{p2}\gamma_2 cos2\Theta_{s2} \\ cos\Theta_{p1} & sin\Theta_{s1} & cos\Theta_{p2} - \Lambda_p W_{p2} cos2\Theta_{s2} & -sin\Theta_{s2} + \Lambda_p W_{p2}\gamma_2 sin2\Theta_{s2} \\ sin\Theta_{p1} & -cos\Theta_{s1} & -sin\Theta_{p2} - \Lambda_s W_{p2}\gamma_2^2 sin2\Theta_{p2} & -cos\Theta_{s2} + \Lambda_s W_{p2}\gamma_2 cos2\Theta_{s2} \end{pmatrix}$$

$$\gamma_1 = \frac{v_{s1}}{v_{p1}}, \quad \gamma_2 = \frac{v_{s2}}{v_{p2}}, \quad W_{p1} = \rho_1 v_{p1}, \quad W_{p2} = \rho_2 v_{p2},$$

$$\frac{sin\Theta_{p1}}{v_{p1}} = \frac{sin\Theta_{s1}}{v_{s1}} = \frac{sin\Theta_{p2}}{v_{p2}} = \frac{sin\Theta_{s2}}{v_{s2}},$$

where $W_{\nu n}$ is the seismic impedance; γ_n is the ratio between shear and compressional velocities; $\Theta_{\nu n}$ is the angle of reflection or transmission; ν shows the type of wave (P, SV); n refers to the number of the medium; and the sign T indicates matrix transposition.

The difference between the systems of equations for the boundary conditions of rigid contact and non-rigid contact is contained only in the addition of 4 elements with non-rigidity parameters into matrix **C**. This fact allows us to easily modify the wave field modeling

computation programs based on the ray theory for complex media with different types of contact at the boundaries.

Note that all transmission and reflection coefficients will be complex-valued for any incidence angle of wave, which means that at the non-rigid contact, not only amplitude, but also phase will change. It can be easily seen from the writing of the reflection and transmission coefficient in the form:

$$K_{\nu 1}^{\varepsilon n} = |K_{\nu 1}^{\varepsilon n}| e^{i\phi}, \quad \text{where} |K_{\nu 1}^{\varepsilon n}| = \text{mod} K_{\nu 1}^{\varepsilon n}, \quad \phi = \text{arg} K_{\nu 1}^{\varepsilon n}, \quad \varepsilon = p, s. \qquad (5)$$

In our study of the dynamic properties of generated elastic body waves, we will, first of all, analyze the behavior of modulus and argument (amplitude and phase) of the reflection and transmission coefficients.

3. NUMERICAL RESULTS

To study the dynamic properties of elastic body waves generated at a boundary with non-rigid contact between two media let us consider two models of elastic isotropic homogeneous media divided by a plane interface:

Model I – a model of media with different values of physical parameters:

v_{p1}= 5.8 km/s, ρ_1= 2.6 g/cm^3, v_{p2} = 6.5 km/s, ρ_2= 2.8 g/cm^3; $v_p/\, v_s$ = 1.73.

Model II – a model of media with the same values of physical parameters - the model of a single fracture in a homogeneous medium:

$$v_p = 6.5 \text{ km/s}, \quad \rho = 2.8 \text{ g/cm}^3, \quad v_p/\, v_s = 1.73$$

(index 1 refers to the upper medium, 2 refers to the lower one).

The results of numerical experiments are given for model I (Figures 1-4) and for model II (Figures 5-6) in modulus and argument curves of reflection and transmission coefficients (expression 5) as functions of the wave incidence angle (α) for different values of the non-rigidity parameters. The coefficient curves were calculated for the 2-D model of media with the boundary condition (2) (Druzhinin and Luneva, 1992). The values for the non-rigidity parameters were chosen as follows: $|\Lambda_p|$=$|\Lambda_s|$=0.; 0.1; 0.5; 1.0 (10^{-6}m^{2}s/kg). These figures demonstrate the general tendency of the reflection and transmission coefficient dependence on the values of non-rigidity parameters and the difference between the reflection and transmission coefficients at the rigid and non-rigid contacts between media.

For the reflected waves, the theory generally predicts an obvious increase in wave amplitude and in phase shift with increasing values of non-rigidity parameters (Figures 1-4). This tendency is independent on the type of the incident wave (P or S) and to the side of the wave incidence (from the medium with a lower value of seismic impedance or from the medium with a higher one). The amplitude of the reflection coefficients can reach the value of 1 in case of monotype waves (PP, SS) and can even exceed 1 in case of converted waves (PS, SP). Thus, the amplitude of the reflected waves can be compared with the amplitude of the incident wave and can be 6-10 times larger than the amplitude of reflected waves produced by the rigid contact between media. The absolute value of the phase shift of the reflected waves changes in the range from 0° to 180°. The behavior of the reflection coefficient curves is considerably more complicated for the incident wave of the SV type (Figures 3-4). For the transmitted monotype waves, the theory predicts a distinct decrease in wave amplitude

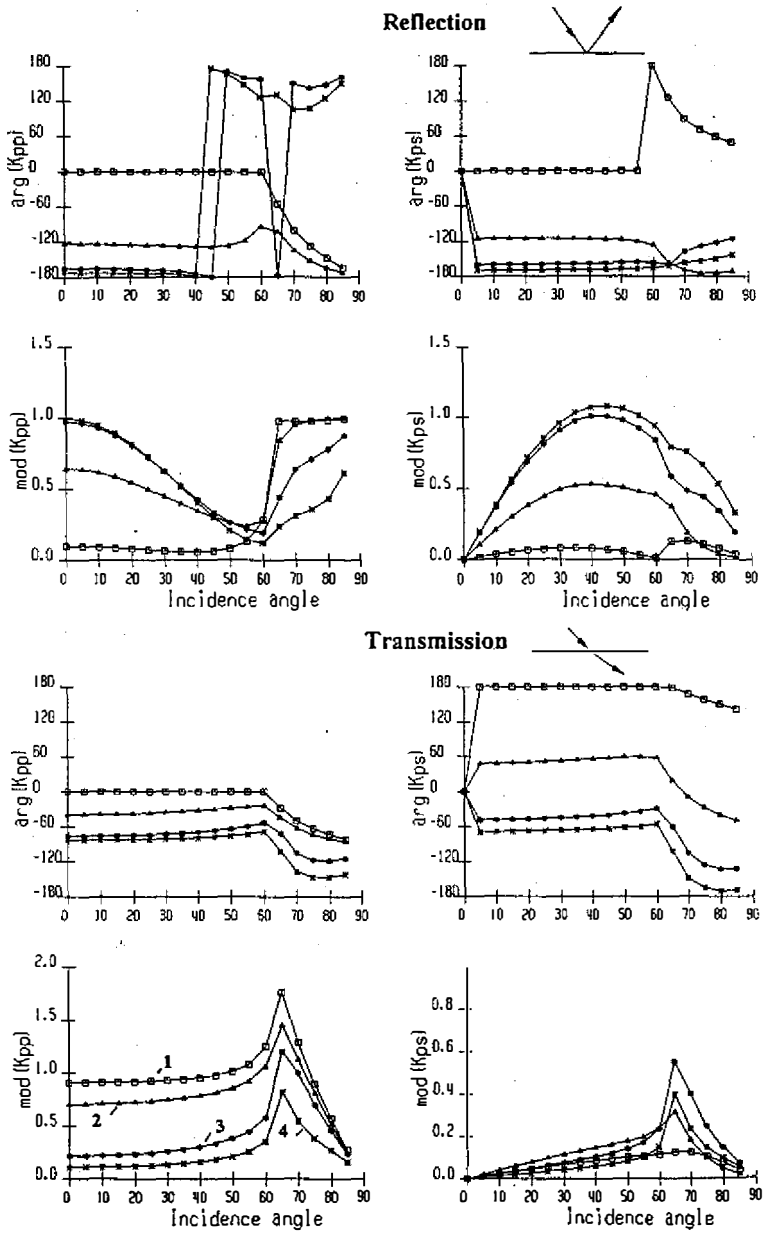

Fig. 1. Dependence of modulus and argument of the reflection/transmission coefficients of seismic waves on the angle of incidence for model I (v_{p1}= 5.8 km/s, ρ_1 = 2.6 g/cm^3, v_{p2} = 6.5 km/s, ρ_2= 2.8 g/cm^3;v_p/v_s = 1.73), non-rigid contact between media in case of the P -wave incident from the upper medium. The coefficients were calculated every 5 degrees of the incidence angle. The curves' signs correspond to the different values of the non-rigidity parameters $\Lambda_p = \Lambda_s(10^{-6}\text{m}^2\text{s/kg})$: $|\Lambda_\nu|$=0. (rigid contact); 2-$|\Lambda_\nu|$=0.1; 3-$|\Lambda_\nu|$=0.5; 4-$|\Lambda_\nu|$=1.0.

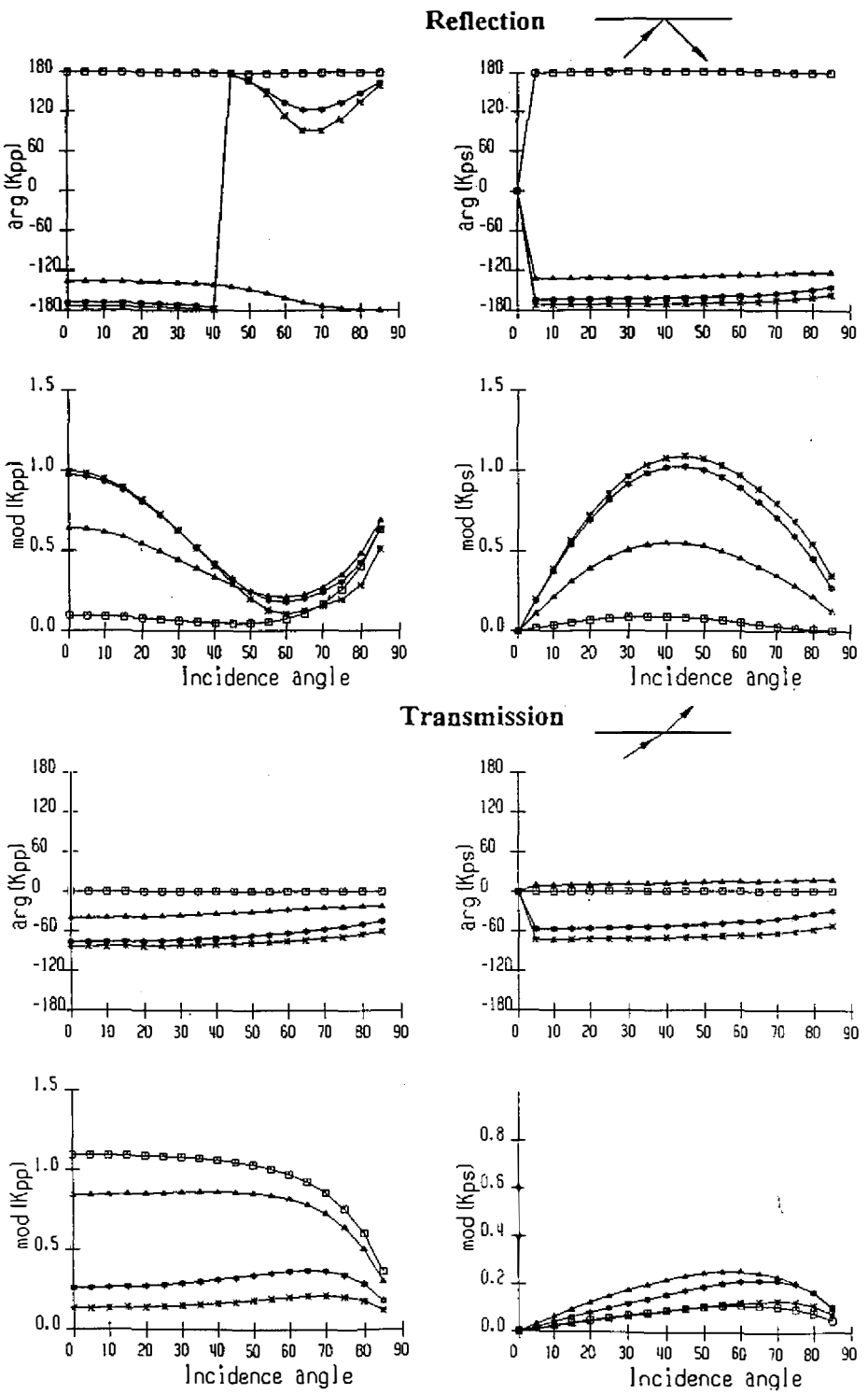

Fig. 2. As in Fig. 1, but for the P-wave incident from the lower medium.

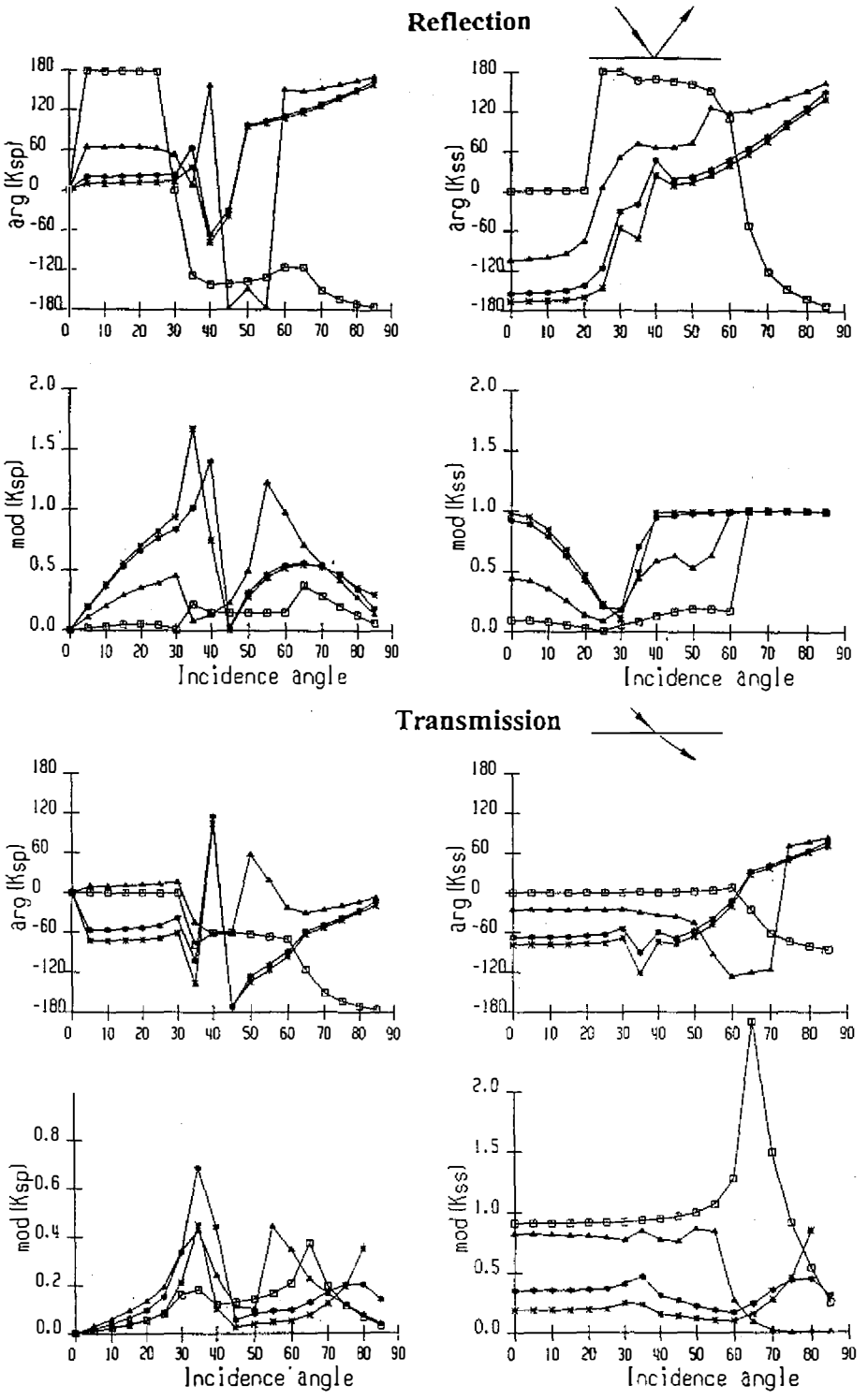

Fig. 3. As in Fig. 1, but for the SV-wave incident from the upper medium.

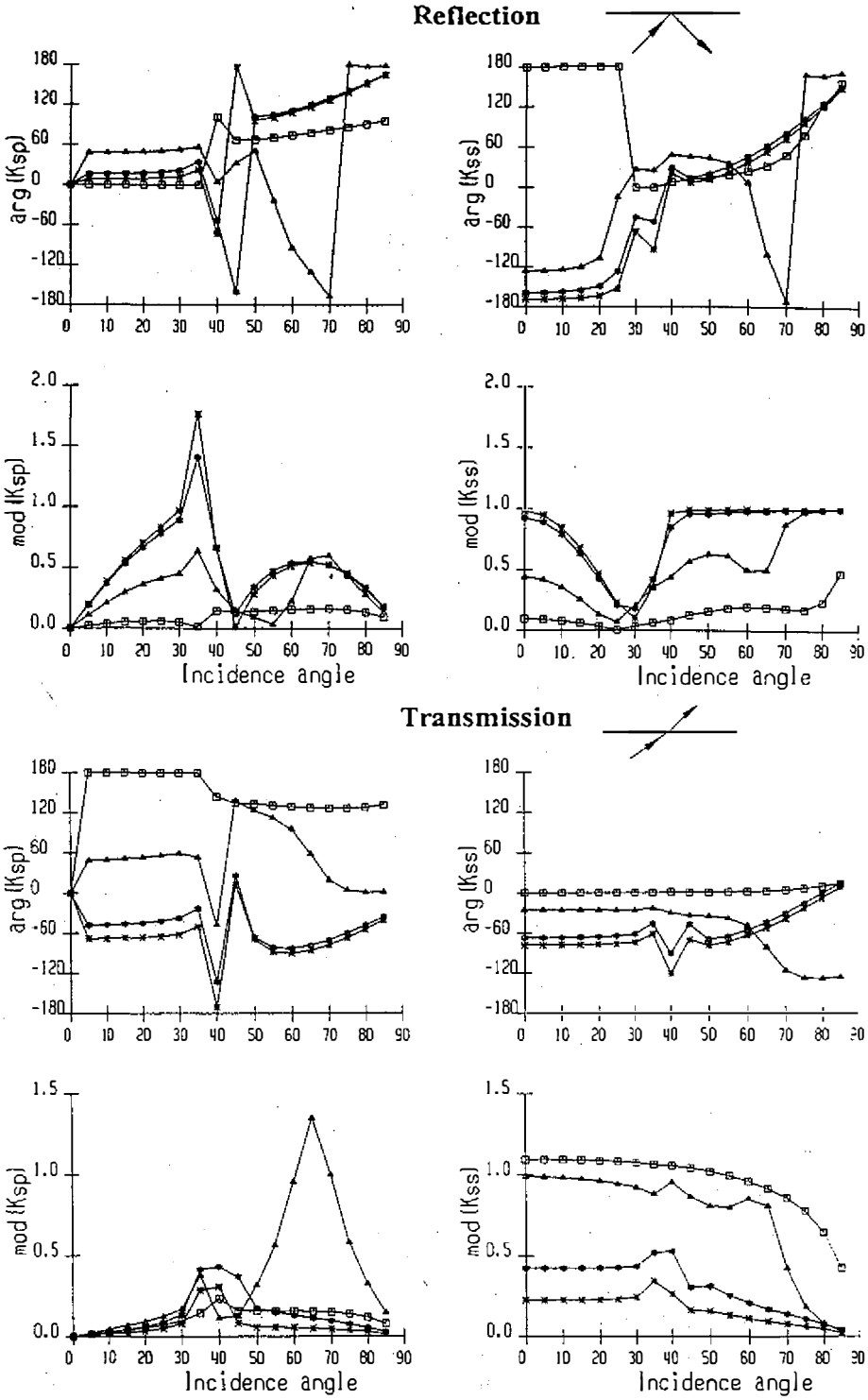

Fig. 4. As in Fig. 1, but for the SV-wave incident from the lower medium.

and an increase in phase shift with increasing Λ_ν (Figures 1-4). But the amplitude of the transmitted converted waves generally increases in 2-5 times with increasing Λ_ν till 0.5 and then decreases. When $|\Lambda_\nu|$ approaches to 1.0, the amplitude of the transmitted waves becomes small enough, about 0.1 of the amplitude of the incident wave. The absolute value of the phase shift of the transmitted converted waves generally increases with increasing Λ_ν.

The behavior of reflection and transmission coefficient curves $K(\alpha, \Lambda_\nu)$ in the critical angle zone can change sharply. For example, in the subcritical zone the curves of (K_{p1}^{p1}) with higher values for Λ_ν have higher amplitude values (Figure 1) gradually decreasing to 0.2 with increasing α till the value of the critical angle is reached (α_{crit}=63°). In the overcritical zone, when $\alpha > \alpha_{crit}$, the amplitude of the reflection coefficient begins to increase with increasing α, but the trend of the amplitude curves K_{p1}^{p1} becomes opposite, i.e., larger reflection coefficient amplitudes correspond to the smaller values of Λ_ν. Another situation is observed in the case of transmitted waves (Figure 1). The amplitude of the transmission coefficient gradually increases with increasing α till α_{crit} and then sharply decreases in consecutive order of the values of Λ_ν. It should be noted that a sharp change of mod[$K(\alpha)$] and arg[$K(\alpha)$] curves occurs at the critical angle ($\alpha = \alpha_{crit}$) synchronously in the case of rigid contact between media. When $|\Lambda_\nu| \neq 0$., the jump in phase shift can begin from different values of α for different values of Λ_ν. In particular, it can be clearly seen in case with reflected waves (Figure 1). When the incident wave is of the SV type, a more complicated behavior of the mod[$K(\alpha, \Lambda_\nu)$] and arg[$K(\alpha, \Lambda_\nu)$] curves is observed as a result that the number of critical angles is more than one. When the incident SV wave goes from the upper medium, there are three critical angles for the investigated model I – $\alpha_{crit}(s1s2) = 63°$, $\alpha_{crit}(s1p1) = 35.3°$, $\alpha_{crit}(s1p2) = 31°$ (Figure 3). When the incident SV wave goes from the lower medium, there are two critical angles - $\alpha_{crit}(s2p2) = 35.3°$, $\alpha_{crit}(s2p1) = 40.3°$ (Figure 4).

Another significant effect of waves generated at non-rigid contact is the distinction of the pulse form among the generated waves to each other and with respect to the pulse form of the incident wave because of their shift difference in phase. In case of a broad frequency band signal of the incident wave, the changes in an apparent period of generated waves should be observed, taking into account the dependence of Λ_ν on frequency. No less important conclusions are drawn from the dynamic analysis of a model of a single fracture, as a special case of non-rigid contact between similar media (model II). A wave incident upon the fracture causes intense reflected waves correlative with the amplitude of the incident one (Figures 5 and 6). When the wave propagates through the fracture, it can generate converted waves, the amplitudes of which are comparable with the amplitudes of monotype waves. But the amplitudes of monotype transmitted waves become weaker than the amplitude of the incident wave. The common behavior of $K(\alpha, \Lambda_\nu)$ for the model of a fracture and non-rigid contact at the boundary (model I) is similar. The difference between them is connected with the ratio of the physical parameter values of contacting media.

As shown above, the character of $K(\alpha)$ dependence on the non-rigidity parameters Λ_ν for the different types of waves is different. Let us stress some important features. The amplitude of reflected waves increases considerably and becomes comparable with the amplitude of the incident wave and even exceeds it. The transmitted converted and transmitted monotype waves can have almost equal amplitudes. These dynamic properties are quite dissimilar from those of the traditional model of rigid contact between media. In practice, the effect of increasing amplitudes of reflected and converted waves could be interpreted

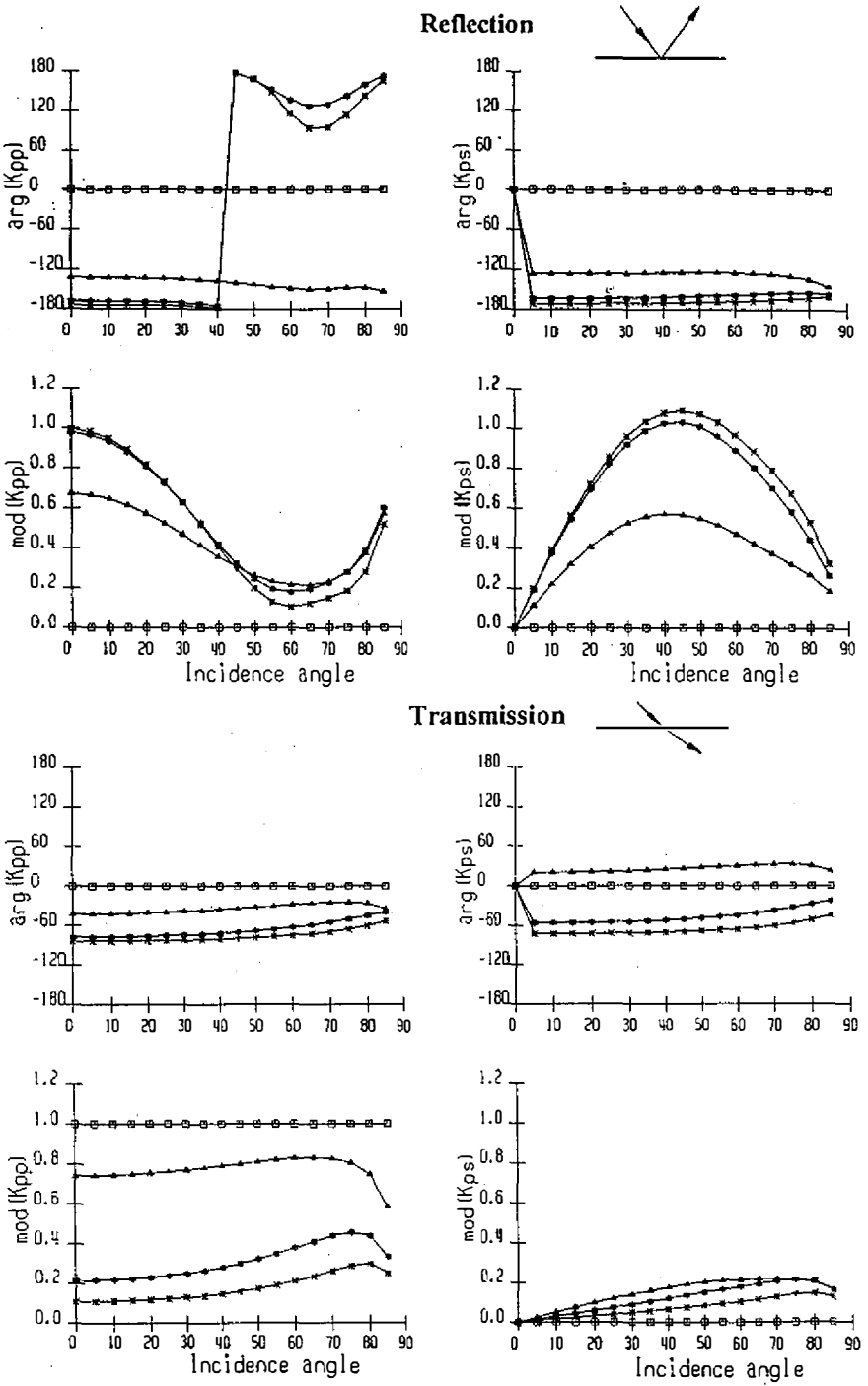

Fig. 5. Dependence of modulus and argument of the reflection/transmission coefficients of seismic waves on the angle of incidence for model II (v_p = 6.5 km/s, ρ = 2.8 g/cm^3, v_p/v_s = 1.73), a single fracture in case of the incident P-wave. The curves' signs are the same as in Fig. 1.

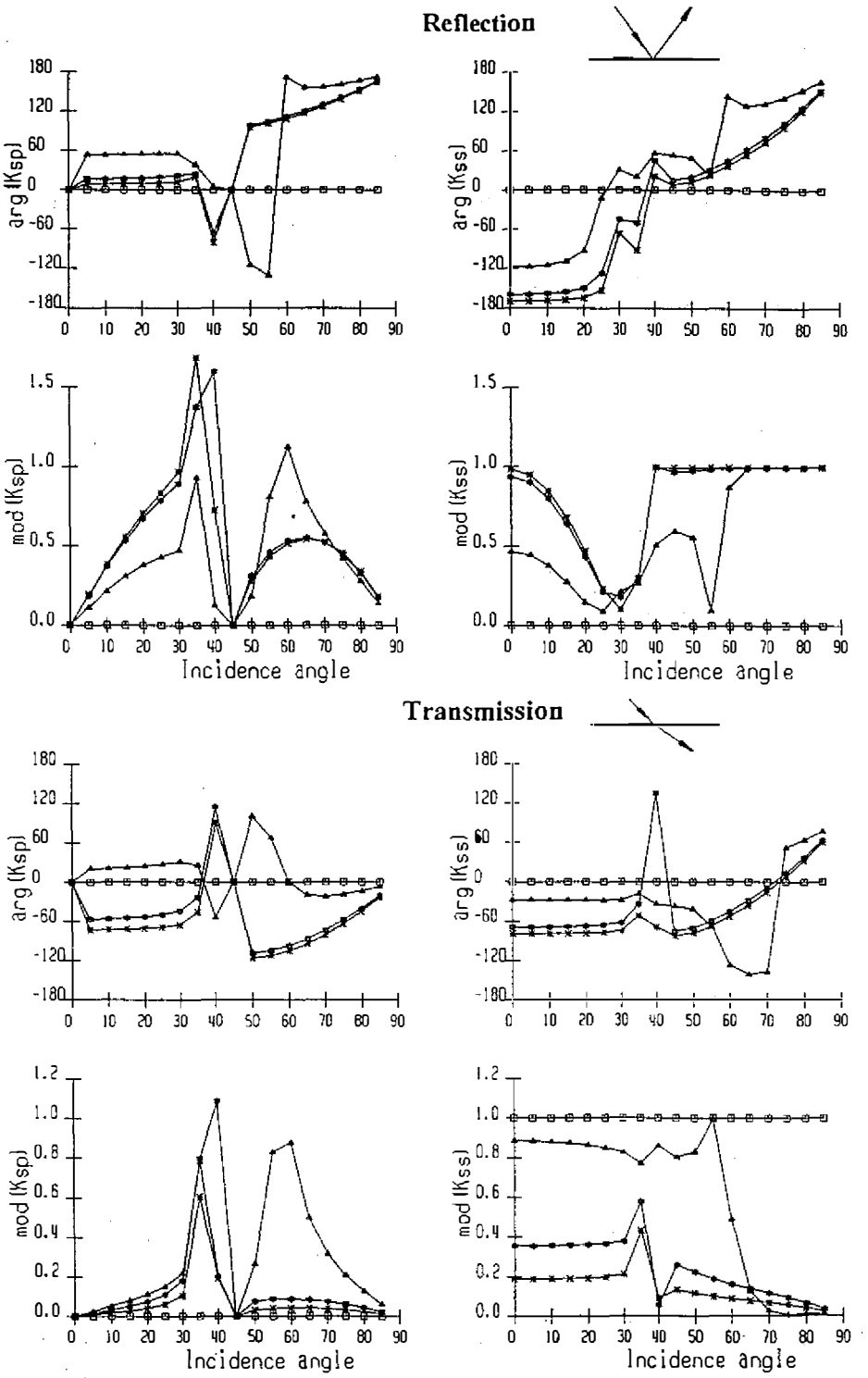

Fig. 6. As in Fig. 5, but for the incident SV-wave.

incorrectly using traditional models as an increase of the ratio of seismic impedances (W_2/W_1) of the contacting media. Another significant dynamic effect - a phase shift or a variation in the polarity of different waves - may be interpreted incorrectly as a velocity inversion at the boundary. Calculating the reflection/transmission coefficient curves with different values for Λ_p and Λ_s, we can draw some conclusions. In fact, the value of $|\Lambda_p|$ ranges approximately from 0. to 1.0. When $|\Lambda_p|$ is larger than 1.0, the coefficient curves approach to the asymptotes. The value Λ_s can change within much broader limits and mainly influences on the shape of the coefficient curves. The analysis of the $K(\alpha, \Lambda_\nu)$ behavior for the models with a different ratio of seismic impedances at the boundary (W2/W1) and with a different ratio of non-rigidity parameters (Λ_p/Λ_s) shows that the values of the reflection and transmission coefficients are proportionally dependent on the ratio of seismic impedances at the boundary and also dependent on the ratio of non-rigidity parameters.

4. EXPERIMENTAL RESULTS

To check the theory and to find the values of the non-rigidity parameters a physical ultrasonic experiment was made for the model of a single fracture. This experiment was performed on a sheet of duraluminium that was cut and filled with plasticine. The physical parameters of the duraluminium were:

$$v_p = 5400 \text{ m/s}; \; v_s = 3100 \text{ m/s}; \; \rho = 2.7 \text{ g/cm}^3.$$

Figure 7 displays a schematic diagram of the experimental model. Two profiles were set up to measure x, z displacement components of the transmitted and reflected waves. On the observation profiles receivers were placed at every 5 degrees of the wave incidence angle. The source of point type that generated compressional waves was located at the beginning of the lower observation profile. The prevailing frequency of the source was 120 KHz corresponding to the wave period of $0.83 \cdot 10^{-5}$s and to the length of the compressional wave λp = 4.43 cm. The thickness of the plasticine-filled layer was about 1 mm, much smaller than λp. The wave attenuation in the duraluminium was negligible.

Before cutting the sheet of duraluminum, the control measurements of the displacements were performed on the upper observation profile to estimate the source amplitude (A_o) and the amplitude variation with distance and from the direction of wave propagation. For our model the displacement of the incident wave at any point ζ can be expressed:

$$u(\zeta, t) = \frac{A_o \cdot f(t) \cdot \psi(\alpha)}{\sqrt{R(\zeta)}}, \tag{6}$$

from where we can single out A_o:

$$A_o = \frac{u(\zeta, t)\sqrt{R(\zeta)}}{f(t) \cdot \psi(\alpha)}, \quad u(\zeta, t) = \sqrt{u_x^2(\zeta, t) + u_z^2(\zeta, t)}, \tag{7}$$

where $u(\zeta, t)$ is the displacement; $u_x(\zeta, t)$ and $u_z(\zeta, t)$ are the x and z displacement components obtained from the measurements; $f(t)$ is the source-time function, and $R(\zeta)$ represents the source-to-receiver distance. The experimentally obtained function $\psi(\alpha)$ defines the amplitude attenuation depending on the angle of wave propagation (α). To decrease the influence of S-polarized wave generated near the source, the surface was covered plasticine

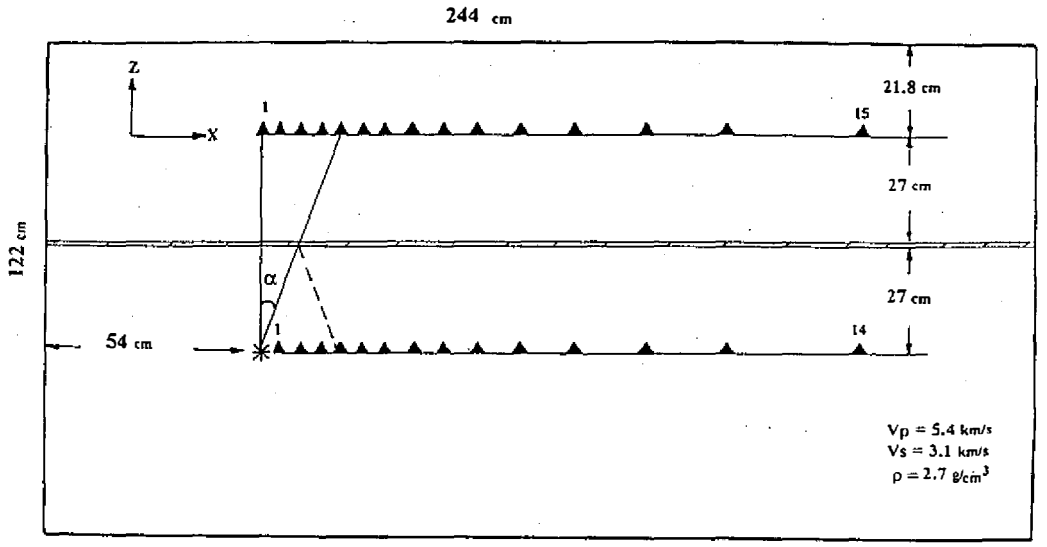

Fig. 7. Schematic diagram of the experimental arrangement of source (asterisk) and receivers (triangles) to measure the displacement of transmitted and reflected waves generated by the plasticine-filled thin layer (double line). On the observation profiles receivers were set up at every 5 degrees of the P wave incidence angle.

in the source vicinity. Using expression (7), we calculated the source amplitude for every observation point and also estimated the average source amplitude $\bar{A}_o$ and relative amplitude variation (ε_i) from the average as follows:

$$\bar{A}_o = \frac{\sum_{i=1}^{15} A_{oi}}{n}, \quad \varepsilon_i = \frac{(A_{oi} - \bar{A}_o) \cdot 100\%}{\bar{A}_o}, \tag{8}$$

where A_{oi} is the source amplitude obtained from experimental data for the observation points with number i. Furthermore, we took a more pronounced second positive phase of the generated impulse $f(t)$ to estimate the wave amplitudes. The measurement error of amplitudes ranges from -10% to 10%. The table shows relative amplitude variations from the average amplitude value:

i	1	2	3	4	5	6	7	8	9	10	11	12	13	14	15
ε_i(%)	-.04	1.7	-1.3	1.5	2.3	.06	6.0	6.1	-5.4	10.	-10.	-5.3	-5.5	4.5	-4.8

The transmission and reflection coefficients as a function of the of incidence angle (α) were obtained from the experimental measurement of displacements in this form:

$$K_{p1}^{\nu n}[\alpha_\nu(\zeta)] = \frac{A_{\nu n}(\zeta)}{\bar{A}_o} = \frac{\sqrt{u^2_{x(\nu n)}(\zeta,t) + u^2_{z(\nu n)}(\zeta,t)}\sqrt{R_\nu(\zeta)}}{\bar{A}_o \psi[\alpha_\nu(\zeta)]}, \tag{9}$$

$$\nu = p, s, \quad n = 1, 2,$$

where ν shows the type of generated wave, and n shows the number of the medium. The angle of incidence $\alpha_s(\zeta)$ and the path $R_s(\zeta)$ of the PS-wave were calculated numerically for all points ζ, because they are different from those of the PP-wave. The results are shown in Figure 8. In this figure , it can be clearly seen that the thin layer generates relatively high reflected waves. The values of the reflection coefficients reach 1.0 and the conversion coefficients have even higher values. When the angle of incidence is above 40°, the converted reflected waves dominate on the records (Figure 9). The obtained transmission coefficients have small values, about 0.1. Unfortunately, the measurement of transmitted wave parameters was complicated by noise (Figure 10). Nevertheless, the common tendency of their dynamics has been traced. The intensities of the transmitted PP and PS waves are almost equal. The second stage of our study was to fit the theoretical reflection and transmission coefficient curves on to the experimental ones using expression (4) with different values for the parameters Λ_p and Λ_s. The result of this fitting is shown in Figure 8, where the moduli

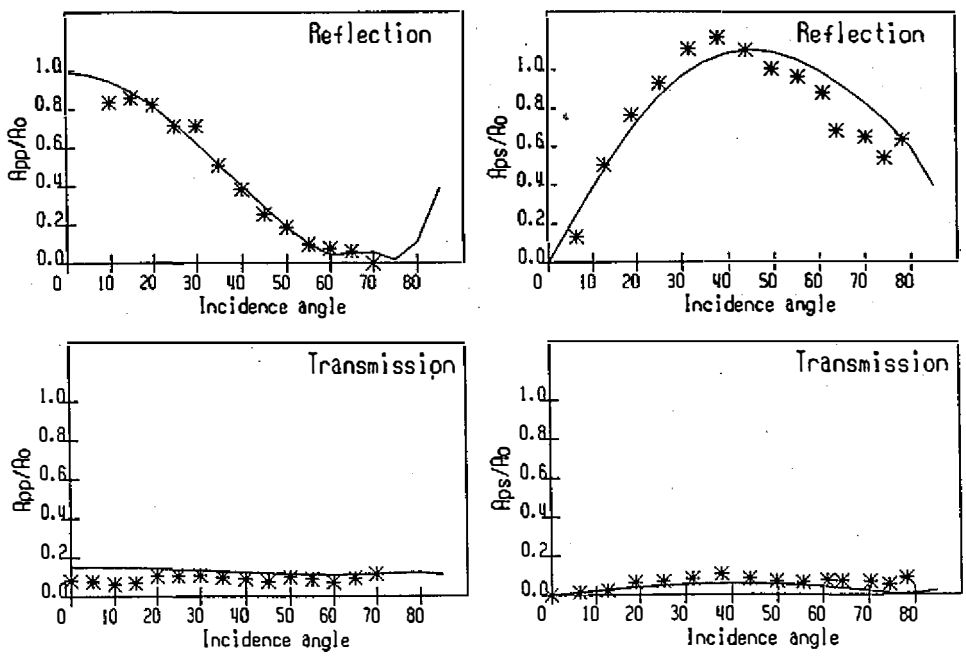

Fig. 8. Transmission and reflection coefficients obtained from experimental data (asterisks) and theoretical transmission and reflection coefficient curves with chosen parameters of non-rigidity $|\Lambda_p|$= 0.9 (10^{-6}m^{2}s/kg), $|\Lambda_s|$ = 6.0 (10^{-6}m^{2}s/kg) (solid curves).

of the parameters have been chosen $|\Lambda_p|$=0.9·(10^{-6}m^{2}s/kg), $|\Lambda_s|$=6.0·(10^{-6}m^{2}s/kg). These calculated data are in good agreement with the observations. By the way, the phase shifts of the generated waves are observed, and their values are about 170° for the reflected waves, about 110° for the transmitted PS-waves, and about -70° for the transmitted PP waves. This is also coincident with the theoretical data. In Figures 9 and 10 it is clearly seen that changes occur in a pulse form of the transmitted wave to each other, and with respect to

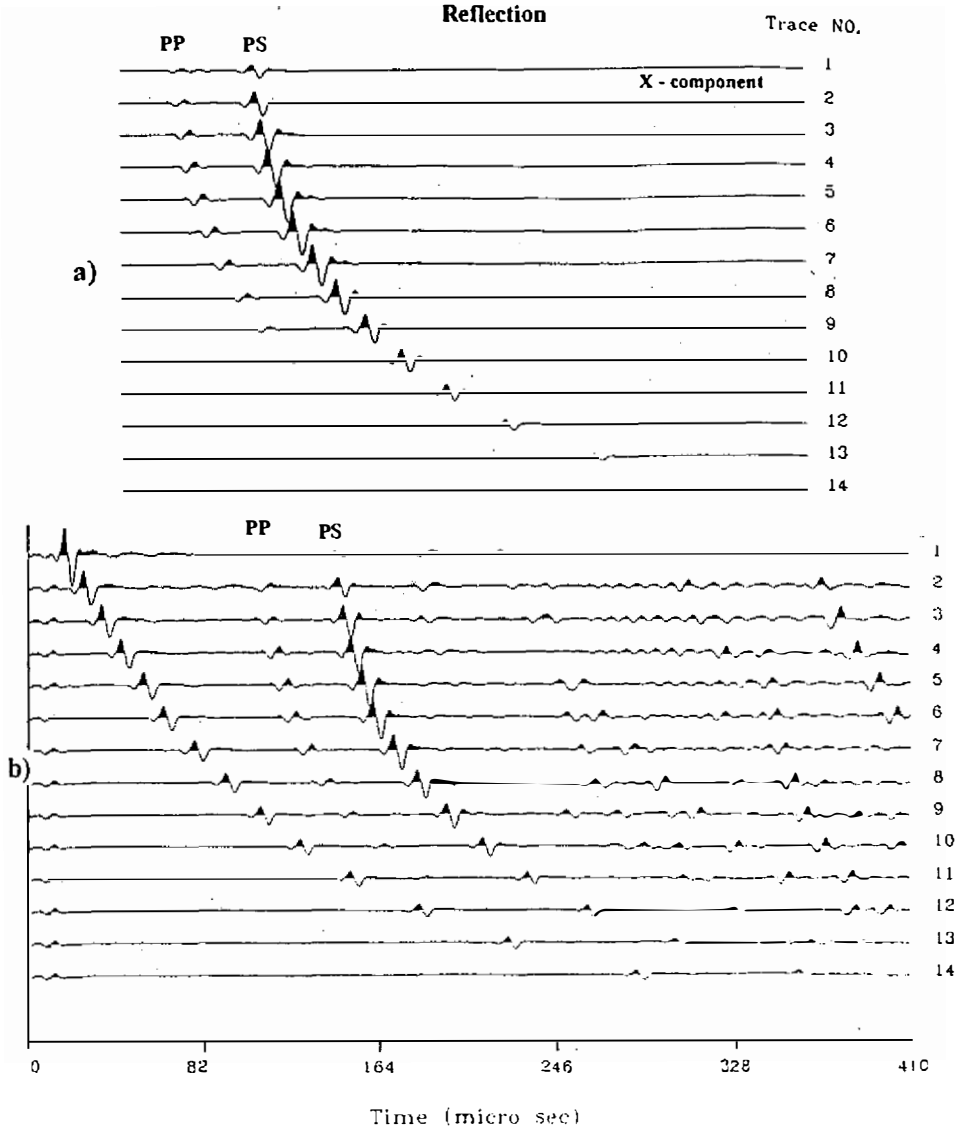

Fig. 9. Synthetic (a) and experimental seismograms (b) of monotype (PP) and converted (PS) waves reflected from the fracture (x-component). Amplitudes are normalized.

the reflected waves, and to the direct incident wave (the first wave in Figure 9). The results of comparison of the theoretical coefficient curves and synthetic seismograms with those obtained from ultrasonic experiments show high level of agreement, and that the parameters of non-rigidity were chosen correctly. The synthetic seismograms were computed taking into account the form of the experimental impulse by means of the method of edge wave superposition (MSEW), that is the original modification of the ray method (Klem-Musatov and Aizenberg, 1989). The wave field computation program based on MSEW for the 2-D complex multi-layered media were made by the first named author.

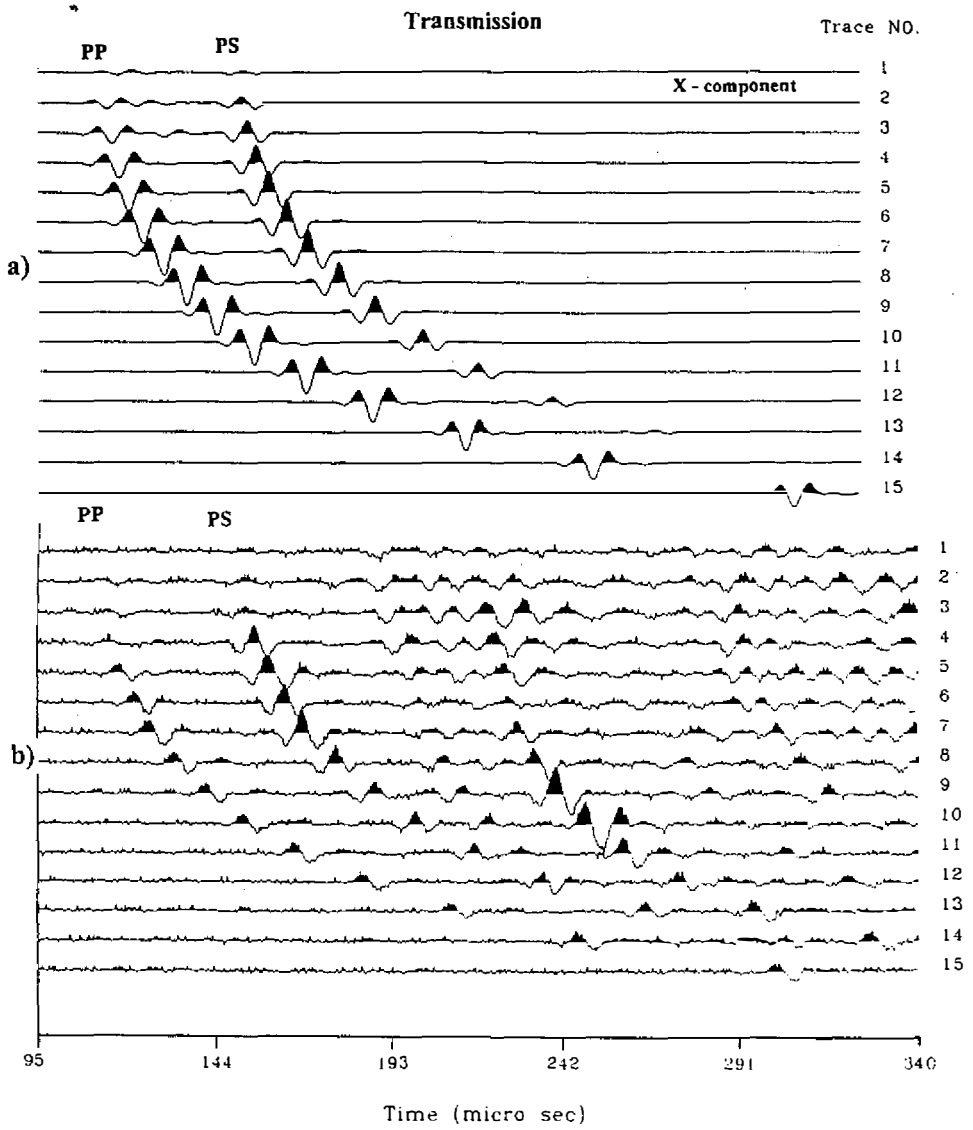

Fig. 10. Synthetic (a) and experimental seismograms (b) of monotype (PP) and converted (PS) waves transmitted through the fracture (x-component). Amplitudes are normalized.

5. CONCLUSIONS

The results of our numerical experiment on the dynamic properties of elastic body waves, generated at the interface of the non-rigid contact between elastic isotropic media, are summarized here. The non-rigid contact generates intense reflected waves. Their reflection coefficients can reach the value of 1.0 and even exceed it. The amplitude of transmitted waves can decrease greatly, even up to 80% relative to the amplitude at the rigid contact.

The amplitude of converted waves may be relatively high and comparable with the amplitude of the corresponding monotype waves. The reflection and transmission coefficients in this case are complex-valued for any incidence angle and frequency dependent. This means that after reflection or transmission the wave always changes phase, and the absolute value of the shift in phase can range from 0° to 180°. The waveforms of the reflected, transmitted and converted waves should be distinguished from each other as a result of the difference of their phase shifts. Generally, the behavior of reflection and transmission coefficient curves depends on the value of the non-rigidity parameters and their ratio and on the ratio of seismic impedance value of the contacting media. A model of a single fracture, as a special case of non-rigid contact between similar media, has been investigated experimentally. The values of the non-rigidity parameters were obtained from the fitting of experimental data. A comparison of reflection and transmission coefficients calculated from the observed data and experimental seismograms with those predicted by the theory shows a high level of agreement.

Acknowledgments The research was supported by the National Science Council under contract NSC 82-0202-M-019-011-Y. During the research period, the first author (M. Luneva) received a NSC Post-Doctoral Fellowship under grant NSC 82-0112-C019-001.

REFERENCES

Aizenberg, A. M., K. D. Klem-Musatov, and E. I. Landa, 1974: The model of anisotropic seismic medium. In: Seismic waves in complex media, Novosibirsk, Nauka, *Siberia Branch*, 64-109 (in Russian).

Brace, W., B. Paulding, and C. Scholtz, 1966: Dilatancy in the fracture of crystalline rocks. *J. Geophys. Res.*, **71**, 3939-3953.

Byerlee, J.,1968: Brittle-ductile transition in rocks. *J. Geophys. Res.*, **73**, 4741.

Druzhinin , A. B., and M. N. Luneva, 1992: Reflection and transmission of seismic waves at the non-rigid contact between elastic isotropic media. *Tihookeanskaya geologiya*, **2**, 141-151 (in Russian).

Hsu, C. J., and M. Schoenberg, 1993: Elastic waves through a simulated fractured medium. *Geophysics*, **58**, 964-977.

Klem-Musatov, K. D., 1965: Investigation of reflection and transmission of elastic waves propagated across fracture. *Fiziko-tekhnicheskie problemi razrabotki poleznikh iskopaemikh*, **6**, 45-57 (in Russian).

Klem-Musatov, K. D., and A. M. Aizenberg, 1989: The edge wave superposition method (2-D scalar problem). *Geophys. J. Int.*, **99**, 351-367.

Kleinberg, R. L., E. Y. Chow, T. J. Plona, M. Orton, and W. J. Canady, 1982: Sensitivity and reliability of fracture detection techniques for borehole application. *J. Pet. Technol.*, **34**, 657-663.

Kozlovsky, E. A.(Ed.), 1984 : Kola super deep drill-hole. Moscow, Nedra, 490pp. (in Russian).

Lutsh, A., 1959: The experimental determination of the extent and degree of fracture of rock focus by means of an ultrasonic pulse reflection method. *S. Afric. Inst. Mining and Metallurgy*, **59**, 412-429.

Malamud, A. S., and V. N. Nikolaevsky, 1989: Earthquakes cycles and tectonic waves. Dushambe, "Donish", p.144 (in Russian).

Nikolaevsky, V. N., 1983: Mechanics of geomaterials and earthquakes. *Itogi nauki i tehniki. VINITI, Moscow*, **15**, 149-230 (in Russian).

Pod'yapolsky, G. S., 1963: Reflection and transmission at the boundary of elastic media in case of non-rigid contact. *Izvestia AN SSSR, Ser. Geophys.*, **4**, 525-531 (in Russian).

Pyrak-Nolte, L. J., L. R. Myer, and N. G. W. Cook, 1990a: Transmission of seismic waves across single natural fractures. *J. Geophys. Res.*, **95, B6**, 8617-8638.

Pyrak-Nolte, L. J., L. R. Myer, and N. G. W. Cook, 1990b: Anisotropy in seismic velocities and amplitudes from the multiple parallel fractures. *J. Geophys. Res.*, **95, B7**, 11345-11358.

Schoenberg, M., 1980: Elastic wave behavior across linear slip interfaces. *J. Acoust. Soc. Am.*, **68**,1516-1521.

Yanovskaya, T. B., and L. A. Dmitrieva, 1991: Influence of non-rigid contact of elastic media on transmission, reflection, conversion coefficients. *Izvestia AN SSSR, Fizika Zemli*, **2**, 45-52 (in Russian).

Yu, T. R., and W. M. Telford, 1973: An ultrasonic system for fracture detection in rock faces. *Can. Min. Met. Bull.*, **66(729)**, 96-101.